Invertebrate Biology 115(3): 191–205.

Advertisement and concealment in the plankton: what makes a copepod hydrodynamically conspicuous?

Jeannette Yen[1,a] and J. Rudi Strickler[2]

[1]Marine Sciences Research Center, State University of New York, Stony Brook, New York 11794-5000, USA
[2]Center for Great Lakes Studies, University of Wisconsin, Milwaukee, Wisconsin 53208, USA

Abstract. *Euchaeta rimana*, a pelagic marine copepod, roams a 3-dimensional environment and its antennular setal sensors are oriented to detect water-borne signals in 3 dimensions. When the copepod moves through water or moves water around itself, it creates a fluid disturbance distinct from the ambient fluid motion. As it swims and hovers, the copepod's laminar feeding current takes the unstable nature of small-scale turbulence, organizes it, and makes the local domain a familiar territory within which signals can be specified in time and space. The streamlines betray both the 3-dimensional spatial location (x, y, z) as well as the time (t) separating a signal caught in the feeding current and the copepod receptor—giving the copepod early warning of the approach of a prey, predator, or mate. The copepod reduces the complexity of its environment by fixing information from a turbulent field into a simpler, more defined laminar field.

We quantitatively analysed small-scale fluid deformations created by copepods to document the strength of the signal. Physiological and behavioral tests confirm (a) that these disturbances are relevant signals transmitting information between zooplankters and (b) that hydrodynamically conspicuous structures, such as feeding currents, wakes, and vibrations, elicit specific responses from copepods. Since fluid mechanical signals do elicit responses, copepods shape their fluid motion to advertise or to conceal their hydrodynamic presence. When swimming, a copepod barely leaves a trace in the water; the animal generates its flow and advances into the area from which the water is taken, covering up its tracks with the velocity gradient it creates around itself. When escaping, it sheds conspicuous vortices. Prey caught in a flow field expose their location by hopping. These escape hops shed jet-like wakes detected by copepod mechanoreceptors. Copepods recognize the wakes and respond adaptively.

Additional key words: crustacean, Reynolds number, signal, sensor, fluid flow

Many planktonic copepods selectively capture certain sizes of prey (see Yen 1985 for an example). Yet motion of the prey can also influence selectivity (Yen 1982). In fact, Strickler & Twombly (1975) pointed out that the expression "size-selective feeding" misrepresents nature. Rather, "Reynolds number selective feeding" more accurately describes the signal perceived by the predator. The Reynolds number, Re, describes not only the ratio of inertial forces to viscous forces but also the kind of fluid disturbance a moving body creates while swimming through the medium (Batchelor 1967). Van Dyke (1981) provides beautiful illustrations of how slight changes in Re produce markedly different fluid signatures around a simple cylinder. As the Reynolds number increases, a remarkable variety of patterns succeed one another: at Re = 0.16, symmetrical Stokes flow (fig. 6 of Van Dyke); at Re = 9.6–41.0, symmetrical standing eddies (figs. 40–46); at Re = 300, a Kármán vortex street (behind the cylinder, with periodic shedding of vortices; first photograph following the title page); and at Re = 2000 and 10,000, turbulent wake (figs. 47, 48).

These variations in flow patterns with changes in Re form the basis of our analysis of zooplankters swimming through water. Zooplankters come in different sizes and shapes, and they swim at different speeds, changing speeds to suit their activity. The effect of the combination of size, shape, and speed on their fluid signature is best expressed in the Re. The Re values of zooplankters range from 0.1 to 1000. At these low Re, small changes in Re can be amplified into large

[a] To whom correspondence should be addressed.

differences in hydrodynamic characteristics. If zooplankters can recognize these differences, they may be able to identify species, gender, age, activity, etc. of the animal that swam through the area before them. Our research addresses questions about these biological-physical interactions.

To distinguish between important fluid signals of mobile prey, predators, and mates, a copepod requires a detection system with morphological precision and acute physiological sensitivity. These crustaceans (1–10 mm long) must perceive small-scale fluid signals above a background of continuous fluid motion. Mechanoreceptive setae along the antennules enable the copepod to detect fluid flow.[1] By bending setae, water flow is transduced into a neural signal and detected by the copepod (Yen et al. 1992). Transduction appears to be facilitated by microtubular structures (Horridge & Boulton 1967; Strickler & Bal 1973; Markl 1978; Friedman 1980; Dourdeville 1981; French 1988; Weatherby et al. 1994). Physiological evidence shows that even submicrometer displacements of antennular setae generate receptor potentials transmitted along the antennule (Yen et al. 1992). A larger displacement elicits a greater number of impulses with shorter latencies, indicating possible coding for signal intensity (Yen et al. 1992). The ability of setae to exhibit graded responses to signals of different intensities (displacements) can be a physiological mechanism for Re selection of different sizes of prey.

As water is in constant motion, the setae on copepod antennules are subject to fluid motions of varying directions and speeds. However, the direction and speed of flow can be restricted by the setal structure and viscous forces. Setae follow flow in the distal direction better than in the proximal direction because the asymmetry in most setal sockets permits distal bends more easily than proximal bends (Boxshall et al. 1997). Flow speeds are strongly attenuated by the viscosity of water. For physically-induced disturbances, viscosity reduces the water motion to eddies similar in size and speed to those created by moving copepods (Mann & Lazier 1991; Osborn 1996). Further reduction of flow speeds occurs when the fluid approaches the boundary layer adjacent to a copepod. The elasticity of the chitin that forms the seta attenuates the speed of setal bends in response to fluid flow. Stiff or short setae buried in the boundary layers will experience smaller displacements than longer or more flexible or feathered setae. Given the diversity noted in the structure of setae (Huys & Boxshall 1991), the copepod sensory system appears capable of perceiving a range of fluid speeds and directions.

To document perception of signals, we can record the behavioral responses of copepods to biologically relevant signals. The copepod has a repertoire of responses, including escape, capture, mate, pause and sink, antennal flick and turns, fast and slow swimming. One of the most obvious movements is the high-speed escape in which the copepod darts quickly through the water over a distance of many body lengths. Using escape as an indicator of signal detection, many studies have shown that copepods can detect fluid deformation (Strickler 1977; Haury et al. 1980; Zaret 1980; Yen & Fields 1992; Fields 1996; Wong 1996). Subtle responses indicate that copepods can detect the presence of a predator (prey copepods slow their swimming: Folt & Goldman 1981), the presence of unflavored particles (particle-feeding copepods change their swimming pattern: Buskey 1984), or the presence of turbulence (copepods change activity patterns: Marrasé et al. 1990; Hwang et al. 1994; copepods change the allocation of time to each activity: Costello et al. 1990). Thus, a mechanoreceptive sensitivity of copepods to fluid flow has been suggested morphologically and demonstrated physiologically and behaviorally.

To extend our understanding of perception by zooplankters, we need to identify and characterize the important signals that elicit specific responses and to determine how an animal can perceive a signal above the ambient levels of noise. These signals and background levels must be analysed at the time and space scales appropriate to the zooplankter sensors. This requires a definition of fluid dynamics at low to intermediate Re, a difficult realm to describe. Furthermore, in order to evaluate the sensitivity of a zooplankter to certain cues, these signals must be simulated to identify the behavioral response elicited.

Fluid flow generated whenever zooplankters move through water has a characteristic species-specific structure, quantifiable by the Re of the fluid movement, the direction of the velocity gradient created by the animal movement, the frequency distribution, and the intensity of energy dissipated in the fluid. Strickler visualized (see Kerfoot et al. 1980) the fluid signature or "footprint" that different zooplankters shed. These small-scale signals are transmitted through the medium, carrying information about their propagator. Other zooplankters respond to the water-borne signals by aggregating, escaping, capturing, mating. What is the nature of these signals? How are they created and transmitted? To what signal strength and temporal/spatial character do the zooplankters respond?

Here we describe the structure of some fluid disturbances generated and perceived by copepods. As was

[1] Although called by the diminutive "antennules," by homology with other crustaceans, the first antennae of copepods are larger than the locomotory second antennae.

the purpose of this symposium, we show how video techniques helped us understand invertebrate feeding biodynamics. Color figures illustrate how optical techniques coupled with videography revealed hydrodynamically conspicuous signals generated by copepods moving through seawater. These techniques allowed us (a) to visualize the structural features of the small-scale (<1 cm) fluid motion and (b) to quantify the kinematic nature of the fluid disturbances, including the velocity gradient, frequency, and duration. We discuss how the fluid flows were analysed and confirmed as relevant signals by assaying the behavioral and physiological responses of copepods to these disturbances.

For most examples, we use the pelagic marine copepod *Euchaeta rimana* BRADFORD 1974, a subtropical carnivore that captures mobile prey. We present evidence that *E. rimana* can generate and detect 3 distinct fluid disturbances: feeding currents, oscillations, and wakes. This copepod can detect water flow with mechanosensitive distal setae (Yen et al. 1992; Lenz & Yen 1993), a paired 4-point array of proximal setae (Yen & Nicoll 1990), and other setae on the antennules. The array comprises two straight setae (on antennular articles 3 and 13) that project anteriorly and two curved setae between them (on articles 7 and 8) that project above and below the plane of the antennule and then curve anteriorly. The setae are oriented to detect three orthogonal components of fluid velocity. *Euchaeta rimana* and its congeners use these sensors to detect and consume certain copepods and fish larvae, showing a high degree of responsiveness to variations in prey size, concentration, type, and movement (Yen 1982, 1983, 1985, 1988, 1991). Congeners select prey similar in size to the second basipodal article of its maxilliped, the food-catching appendage. However, when offered prey of the preferred size, they will capture more of the continuously swimming *Pseudocalanus* sp. than the intermittently swimming *Acartia clausii* (Yen 1985). Also, they will eat only live, mobile prey (Yen 1982). Feeding rates do not change even when crushed prey juices are added to mask the chemical signals, and feeding rates are higher in the dark than in the light (Yen 1982). These results suggest that hydrodynamic signals made by the prey are more important than chemical or visual signals. The perceptive field in which the copepod detects its prey extends up to 2 body lengths from the antennular sensors. Without prior contact, the predators lunge accurately, overtaking and capturing the escaping prey (Doall 1995; Yen, unpubl. obs.). Detection of hydrodynamic signals by the copepod is indicated by distinct behavioral responses such as antennal flicks, captures, escapes, or variations in swimming patterns.

Euchaeta rimana and its congeners are lipid-rich biomass dominants in several aquatic habitats, important in the marine food web and found often in the diet of fishes. We present here a study of how this species creates fluid signals that dissipate quickly enough to avoid detection by prey or predators yet remain distinct enough to allow mate recognition. An understanding of signaling processes of this dominant copepod may provide the framework to ask whether other, less abundant species—confined in time to seasonal peaks in abundance, or confined in space to low-energy 'quiet' habitats (the deep sea) or high-energy 'noisy' regimes (coastal waters)—are so limited because of suboptimal sensor acuity or hydrodynamic conspicuousness.

Methods

Velocity gradient of small-scale fluid flow. We used fixed-frame, 3-dimensional videography, based on the moveable frame design of Strickler (1985), to track 20-μm particles entrained in fluid flow. Particles were illuminated by He-Ne laser (630 nm), and particle tracks were recorded in the 60 fields/s S-VHS video format. The x, y, z, t coordinates of the particles permitted analyses of fluid velocity. Over 1000 particle velocities were measured to reconstruct the structure of the feeding current (for details, see Fields & Yen 1993).

Frequency of appendage movements. The speed of the rapid movements of copepod limbs was estimated from kinematic analyses of high-speed films taken at 500 fps (Strickler 1977, 1984; Alcaraz & Strickler 1988).

Visualization of copepod wakes. Visualization of fluid disturbances generated as copepods moved through a smooth density gradient was accomplished using a Schlieren optical path (Strickler 1975a,b, 1977; Kerfoot et al. 1980; Strickler et al. 1995; Strickler & Hwang 1996).

Copepod collection and maintenance. Surface-dwelling *E. rimana* and deepwater *Pareuchaeta* sp. were collected from subtropical seas off Hawaii at the Natural Energy Laboratory of Hawaii Authority (NELHA) via an Ocean Thermal Energy Conversion system of pipes, 0.5 meter in diameter with intakes at 30 m and 600 m (see Fields & Yen 1993). Copepods thus collected are in excellent condition, with intact antennular and caudal setae. These lively copepods were used either immediately in the fixed-frame videography system or in the high-speed cinematography system that we set up at NELHA. Only fresh animals, tethered within a few hours to no longer than a few days after collection, were recorded. For the wake visualization of free-swimming copepods, copepods

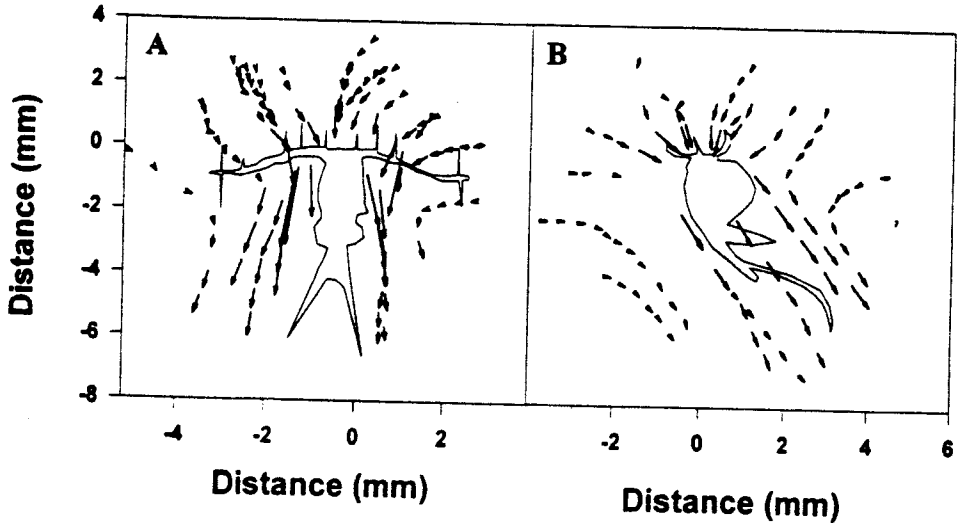

Fig. 1. Trajectories of 10-μm particles entrained within the feeding current of a tethered copepod, *Euchaeta rimana* (adult female, cephalothorax 2.4 mm long). **A.** Plan view (dorsal or ventral) depicting flow direction in a plane parallel to that of the antennules and the straight anteriorly-directed long setae of the antennules. **B.** Profile view (lateral) depicting flow over the dorsal (at left) and ventral (at right) surfaces of the copepod. The (0,0) location is the tip of the rostrum, between the paired antennules. Each arrow represents 1/6 s of particle travel time.

were collected at NELHA, placed in seawater-filled sealed plastic containers, and sent in insulated boxes directly by air cargo to the Strickler laboratory at the University of Wisconsin.

Results

Feeding current of *Euchaeta rimana*

The trajectory of particles entrained in the flow field of *Euchaeta rimana* is depicted in Fig. 1. The speed of the flow varies from 1 to 20 mm s^{-1} intersecting a cross-section of the copepod varying between 0.1 mm (width of antennule) to 2 mm (width of body), giving Re estimates of 0.1 to 40. These low to intermediate values for Re indicate that viscous forces are dominant over most of the feeding current. Close analyses of the pathlines show they do not cross, confirming that the flow regime is laminar within this field.

Within the feeding current, the capture volume can be defined in part by the breadth of the extension of the predator's maxillipeds, which are the capture appendages (Fig. 2A). Within the capture volume, the orthogonal conformation of the 4-point array positions the setae to intersect flow from several directions. Oscillations of the streamlines can be perceived by setae parallel to the streamline and fluctuations in the speed of the flow in the direction of its advance (acceleration) can be perceived by the curved setae perpendicular to the streamlines. Outside the capture volume, most setae are aligned parallel to streamlines of the feeding current and are best for detecting side-to-side oscillations perpendicular to the long-axis of the seta (Tautz 1979). Outside the feeding current, the distal tip of the antennule bears a tuft of setae of varying length, flexibility, and orientation. This tuft of setae can follow a range of flow speeds and directions. By extending the distal tip outside the self-generated feeding current, the strategically placed setal sensors can detect signals in fluid flow outside the animal's control. These include signals made by a predator's feeding current or by small-scale turbulence, for example.

By connecting points of equal speed, a map of the isotachs surrounding the copepod shows complexity in its hydrodynamic structure with strong definition (Fig. 2B,C). A high-velocity zone surrounds the antennae, the locomotory appendages primarily responsible for generating the feeding current. The flow speed is greatest near the antennae (16–20 mm s^{-1} flow region: yellow isotachs) and declines steeply lateral and dorsal to this central region. The left-right symmetry (Fig. 2B) with vorticity of opposite sense (Yen et al. 1991) can contribute to the observed stability of the position of the copepod. The structure of the feeding current mirrors the bilateral symmetry of the body. The flow field structure (Fig. 2C) shows dorsal-ventral asymmetry. The solid dorsal surface of the copepod is more curved, while ventrally, the appendages of the cephalothorax direct the water in close to the body for examination of its content. High flow speeds over the back of the copepod are directed and propelled by the exopod of the biramous antennae. When hovering in its upright position, or in the free-swimming orienta-

tion (see Fig. 3D), the copepod body can be moved dorsally by large flow speeds over the dorsal surface.

The above discussion refers to the feeding current of a tethered copepod, as tethering permitted detailed analyses of the flow field structure in *E. rimana*. Tethering simulates the naturally occurring behavior of hovering in this species. The shape and speeds of the flow field of a tethered copepod are similar to the velocities and curvature of a hovering untethered copepod (Yen et al. 1991). Fields (1996) also compared point measurements in flow fields of 2 other copepod species and found no difference in the water flow velocities in the same positions around tethered vs. untethered copepods. In following sections, signals produced by freely swimming animals are examined using untethered subjects.

Vibrations

Reciprocating appendages can produce vibrations—by a continuous, repetitive movement or as a single cycle of movement. In either case, a frequency can be calculated as the inverse of the cycle's period. The frequency of oscillation has been measured most often in head appendages, as it is these appendages that beat most continuously. From the high-speed films taken of tethered copepods, the beat frequency of the antennae of adult females of *E. rimana* is 70–80 Hz. Its frequency falls within the range noted for most copepods, extending from 1 Hz to 150 Hz (Gill & Poulet 1986; Price & Paffenhöfer 1986). The oscillating antennae of a large (4–6 mm) deepwater subtropical copepod, *Pareuchaeta* sp., are large enough to create conspicuous "ripples" in the Schlieren image, representing water packets moved at a specific frequency by the antennae (Fig. 2D). The oscillation has a frequency of ~30 Hz, similar to the beat frequencies of antennal movements (10, 25, and 38 Hz) noted for a copepod of similar size, *E. antarctica* (Montgomery & Macdonald 1987). The self-generated feeding current signal can be conceptually decomposed into the vibratory AC component (containing an acceleration component) and a net DC flow as described for fishes (Jansson et al. 1990). The DC flow of the copepod feeding current is generated by oscillating head appendages.

The frequency of movements of various copepod appendages differ from each other. Antennules of *E. rimana* complete a single sweep in 80–90 ms, equivalent to 11–12 Hz. Maxilliped extension, part of the capture response, occurs within 25 ms, or at 35–45 Hz. A urosome rears up to its maximum bend and closes down on the swimming legs within about 80 ms, or at 10–15 Hz for the completed movement. The swimming legs can maintain a high-speed escape by multiple thrusts at 35–45 Hz. Other copepods show swimming leg beat frequencies of 50 Hz (Strickler 1975a).

Wakes of escaping copepods

As escaping copepods jump through water, they leave a hydrodynamically conspicuous wake. A freely swimming adult female of *E. rimana* (cephalothorax 2.4 mm long) jumped 3 times and each time, a toroidal vortex was shed (Fig. 3A). A juvenile (cephalothorax 1.5 mm long) jumped 4 times, shedding vortices separated by 3 times their vortex radius (Fig. 3B). Each time, a tiny vortex was created of the same sense (clockwise in this view). The adult stage created a series of vortices at a rate of 30 Hz (Fig. 3A) while the multiple vortices spun off the synchronized motions of the thrusting swimming legs and undulating body of the escaping juvenile had a frequency of ~100 Hz (Fig. 3B). The frequency of the swimming leg oscillations matches the dominant frequency of the animal's wake.

Wakes of freely swimming copepods

In the wake of a freely swimming individual of *E. rimana*, barely a trace is left in the water, as seen in both plan view (dorsal or ventral, Fig. 3C) and profile view (lateral, Fig. 3D). In both plan and profile views, only the distal tips of the antennules and caudal setae create a hydrodynamic trail in the water. The slight sideways (left) drift of the copepod also left a disturbance. However, in the profile view, only the narrow trail of the caudal setae can reveal where the copepod has been.

Discussion

The feeding current as a sensory field

Within the feeding current of *Euchaeta rimana*, flow velocities vary from 1 to 20 mm s^{-1}. The flow field is similar to that of *Eucalanus crassus* (fig. 2 in Strickler 1982) which has a Re of 0.75. At this low Re, flow is laminar. The copepod takes the unstable nature of ambient fluid motion and organizes it within its feeding current. The feeding current entrains water from a discrete sector that follows streamlines along predictable paths. Certain paths converge from 3 dimensions onto the linear array of setae along the paired antennules. Receptors, activated by hydrodynamic signals or prey contact, mediate responses that are directed to that receptor's sector of the feeding current. The copepod may reorient itself so that the streamline intersects its mouth, if the signal is that of prey, or the copepod may initiate an escape in the opposite direction, if the

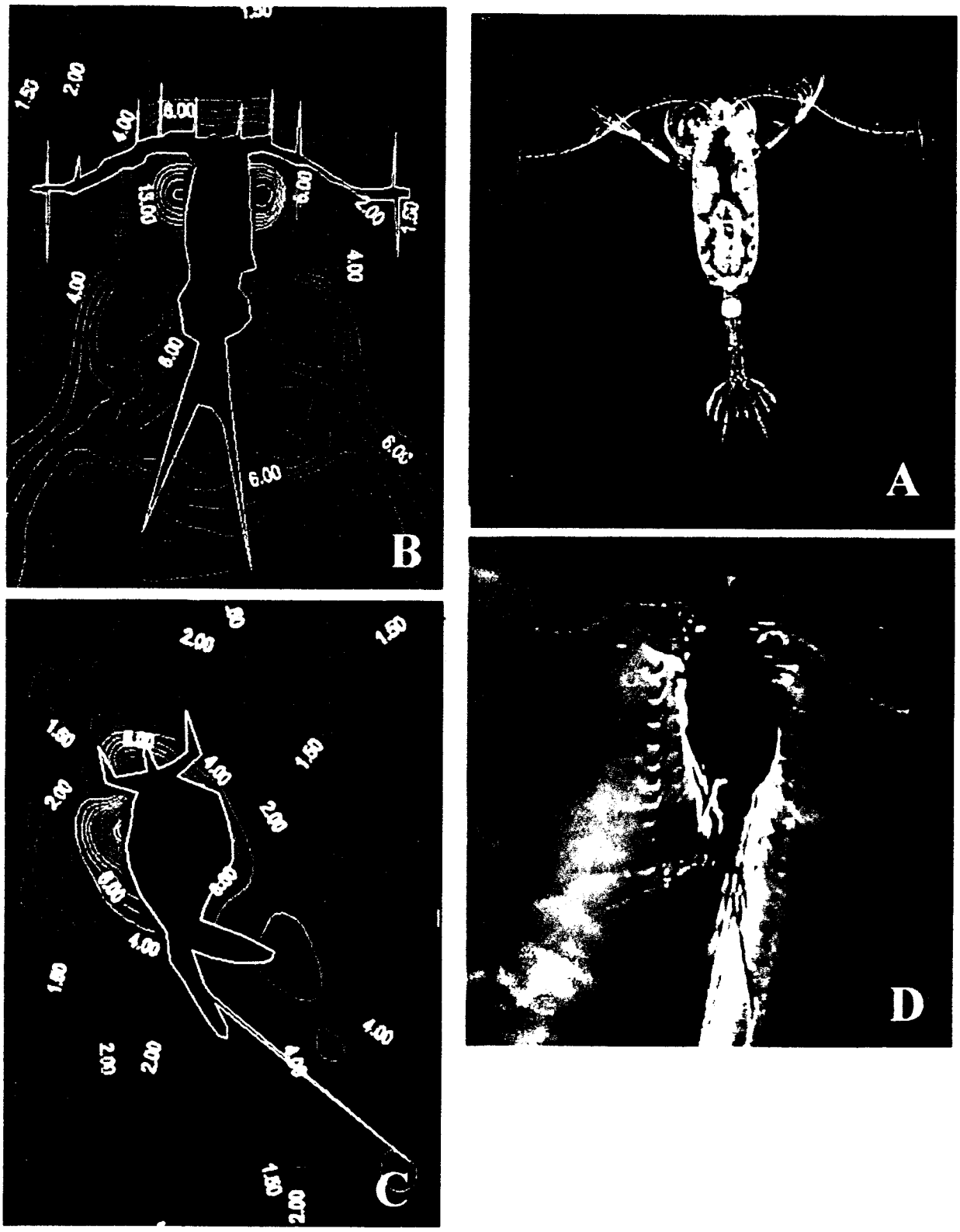

Fig. 2. A. Photomicrograph of a live copepod, *Euchaeta norvegica*, showing the breadth of the extended maxillipeds, captive appendages of this pelagic marine carnivore (cephalothorax ~ 4 mm long). Note the long setae frame the antennules, the pair of very long caudal setae, and the setae imparting iridescence to the caudal fan. Mating occurs with the paired

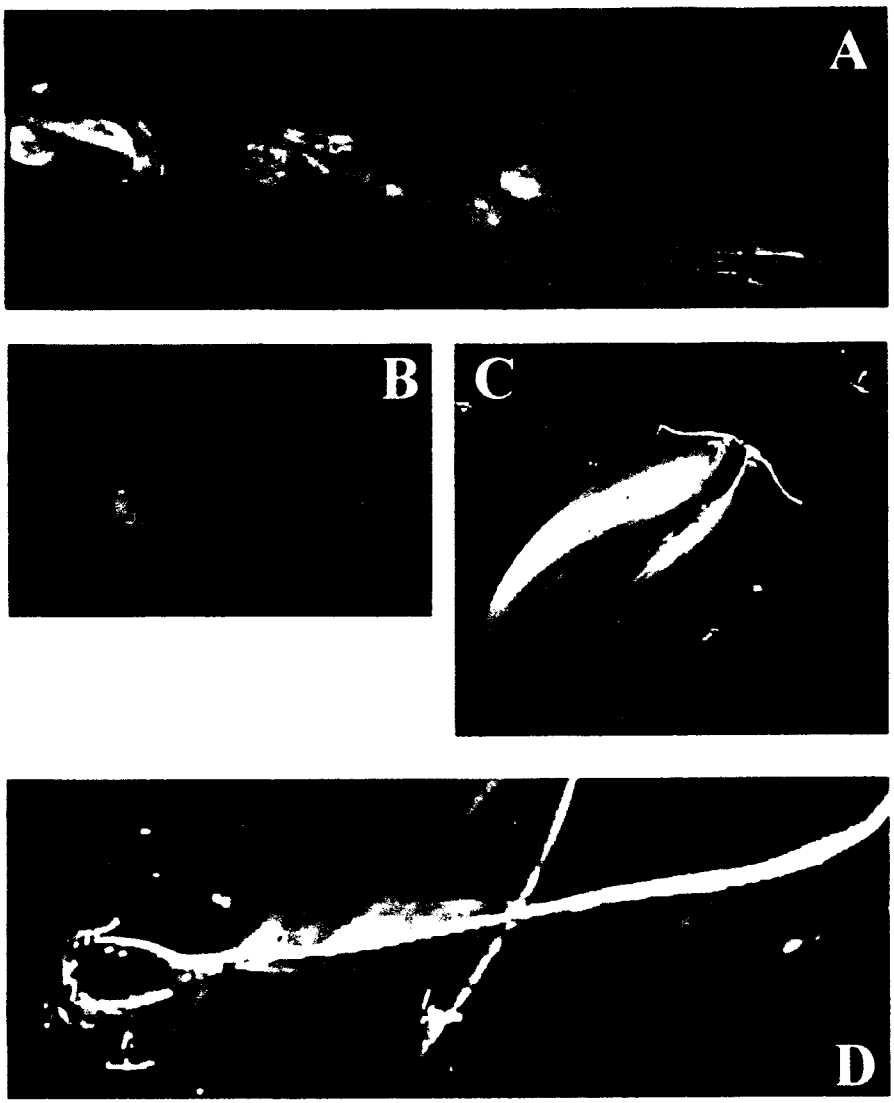

Fig. 3. A. Three toroidal vortices (30 Hz) shed by the escape movements of an adult copepod, *Euchaeta rimana* (cephalothorax 2.4 mm long; copepod is the dark silhouette in the lower right corner). **B.** Four vortices (100 Hz) of clockwise sense shed by the escape movements of a juvenile copepod, *E. rimana* (cephalothorax 1.5 mm long; copepod is seen in profile in the upper left area of the videoimage). **C** and **D.** Wakes of free-swimming copepods, *E. rimana* (cephalothorax 2.4 mm long), swimming through seawater. **C.** Plan view of copepod swimming upward. **D.** Profile view of copepod swimming to the left. Note how smooth and thin the hydrodynamic trail is. The density gradient in the seawater, necessary for Schlieren photography, is enhanced visually with the color gradient. The white image shows the water moved by the copepod into an adjacent layer of water of differing density.

signal is that of a predator. Like a spider and its web, the copepod and its feeding current can be examined as a unit, as recommended by Strickler (1985). Vibrations transmitted along the web inform the spider of the position of the signal source within its web. Signals entrained along the streamlines and intersecting certain receptors inform the copepod of the position of the source within the volume of its feeding current.

Within the copepod feeding current, flow velocities remain relatively stable. Using metabolic energy to

---

oviducts in the translucent body of the copepod are deep blue. **B** and **C.** Isotachs (lines of equal speed) of fluid flow surrounding a tethered copepod, *Euchaeta rimana* (cephalothorax 2.4 mm long). Each isoline represents increments of 1 mm s^{-1} of flow speed (except for the 1.5 to 2.0 mm s^{-1} isolines). **B.** Dorsal view of flow. The innermost yellow isoline of the plan view represents a maximum velocity of 2.0 mm s^{-1}. The blue isoline crossing the distal tip of each antennule represents 1.5 mm s^{-1} flow. These are separated by only 2 mm. **C.** Lateral view of the flow. The innermost yellow isoline on the dorsal side of the copepod body (at left) represents 1.7 mm s^{-1} flow. **D.** Schlieren videoimage of *Pareuchaeta* sp. showing the hydrodynamic imprint left by oscillatory movements of the locomotory appendages, the second antennae. The frequency of the movement is 30 Hz. The distance between ripples (9 ripples per cephalothorax length) is approximately 500 μm. The density gradient in the seawater, necessary for Schlieren photography, is enhanced visually with the color gradient. The white image shows the water moved by the copepod into an adjacent layer of water of differing density.

generate the flow field, the copepod creates its own familiar territory. The organized structure of the copepod feeding current is different from the ambient flow field, which may include small-scale turbulence. At the scale of the copepod, turbulence still exists, though viscosity reduces it to laminar shear. The laminar shear features are thought to be randomly oriented or isotropic. Recently, however, Squires & Yamazaki (1993) did a direct numerical simulation of small-scale turbulence and found that some defined structures have a lifetime and occupy a space but the features still have a degree of randomness not found in the feeding current. Perturbations in the laminar feeding current, now the familiar territory of the copepod, can alert the copepod of an intrusion. Teyke (1988) found that fishes, by swimming at a steady velocity, create a familiar flow field for these same reasons. The strength of the flow field can be controlled by the animal's swimming speed. Any perturbations in the established flow field alerts the fish to the presence of an intruder. The identity of the disturbance—prey, predator, mate, rock—can then be investigated.

The structure of the feeding current is complex, yet defined. Different copepods have feeding currents of different structures (Fields 1996). Within the flow field defined by isotachs, setae assume species-specific orientations with respect to the direction of flow, and different species may have very different arrangements of setae. *Euchaeta rimana* swims with its antennules directed into water not yet disturbed by its own movements or hovers and pulls water in a cone enveloping the entire paired setal array. Hence, the cup formed by the setal array intersects the bulk of the flow so that fluctuations can be perceived and localized. Such an orthogonal sensory array is useful for copepods that roam a 3-dimensional aquatic environment. Responses of these sensors may mediate how copepods orient to signals embedded within the ambient small-scale turbulence. *Pleuromamma xiphias* has mostly anteriorly directed, straight setae oriented on a plane parallel to flow created during the rapid vertically upward swimming and downward sinking phases in its swimming pattern (Fields, pers. comm.). Some species of *Acartia* have a stellar setal arrangement (Chacon-Barrientos 1980; Jonsson & Tiselius 1990) that intercepts flow created when the copepod hops up and sinks in seemingly random orientations. Many antennular setae bend only distally (Boxshall et al. 1997) and are directionally sensitive (Yen et al. 1992). The array of setae on the copepod antennules are multidirected and thus may be used to receive and analyze signals from several directions independently (Strickler & Bal 1973; Friedman 1980; Yen & Nicoll 1990; Weatherby et al. 1994). Such directional orientation and sensitivity may be used to localize the source of the disturbance created by prey, predator, or mate and enable the copepod to differentiate the signal from background noise.

Maintaining a stable familiar environment is necessary for the important functions of sensing signals and food within this scanning field of the copepod. Yet the stability of the feeding current could be disrupted by physically-induced turbulence (see illustrations in Strickler 1985). To evaluate the stability of the copepod feeding current, we can consider (a) the strength of the feeding current, (b) mathematical models of small-scale fluid flow, and (c) the persistence of the flow structures. Considering the strength of the feeding current as a function of the steepness of the velocity gradient or shear, the copepod feeding current has shear that is more intense at a smaller length scale than most small-scale ambient turbulence (Yen et al. 1991). The copepod should be able to maintain its feeding current in the face of small-scale turbulence. Kiørboe & Saiz (1995) comment that only under conditions of vigorous mixing can small-scale turbulence erode the copepod feeding current. Squires & Yamazaki (1993) modeled small-scale turbulence by a direct numerical simulation implementing the Navier-Stokes equations of motion, and Stein et al. (1994) modeled the fluid flow in the copepod feeding current. By merging these two mathematical models, we could place the organized copepod current within the small-scale turbulence field and define conditions where turbulence can interfere, disrupt, or overwhelm the copepod feeding current. Such a model could examine the degree of organization the copepod's feeding current can impart to the unstable fluid motion of turbulence. Consideration also should be given to the persistence of these fluid structures. Using metabolic energy, the biologically-generated feeding current is relatively constant while the physically-induced eddies are transient and are constantly losing energy at this end of the Kolmogorov cascade. An ephemeral eddy may momentarily erode the feeding current but the copepod can rebuild it. The copepod can re-establish its familiar territory within a time interval proportional to the force of propulsion of the antennae driving the feeding current. The individual eddy will continue to dissipate and fade.

Prey-predator signals within the feeding current arena

A copepod's feeding current entrains signals. Odors that become entrained within the feeding current get stretched and sheared but stay within the streamlines—discrete in space, defined in velocity. A phycosphere, surrounding an algal cell, can be separated from the

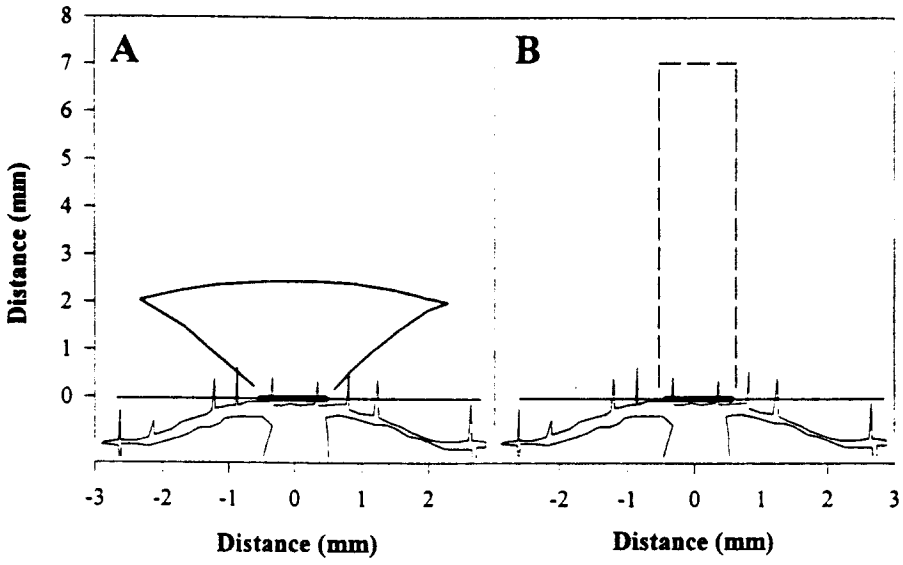

Fig. 4. Comparison of the amount of water scanned by hovering (**A**) vs. free-swimming (**B**) adult females of *Euchaeta rimana* (cephalothorax 2.4 mm long). The shape enclosed by the solid (cone in **A**) and dotted (rectangle in **B**) lines is the calculated area intersected by the central proximal region of the paired antennules (dark bar = 1.0 mm width) within one second by the copepod hovering (**A**), generating a feeding current with flow velocities as depicted in Fig. 1, and by the copepod freely swimming at 7 mm s^{-1} (**B**).

cell if water is entrained in advective flow (Lazier & Mann 1989). This occurs within the sheared flow of a copepod feeding current. The leading edge of the deformed phycophere reaches the copepod before the cell, stimulating aesthetascs to recognize important chemical signals. From its familiarity with the spatial distribution of streamline paths and their associated velocities within the feeding current, the copepod may be able to determine the time and distance separating the signal source from the sensor. This capability of remote detection gives the copepod early warning of the approach of the cell. Koehl & Strickler (1981) visualized a dye stream of alga-bearing water parcels diverted actively by the copepod. Andrews (1983) modeled this mathematically, and Moore et al. (1994) traced it electrochemically. This variety of methods confirms the spatial integrity of the signal within the streamlines of the feeding current. Asymmetric movements of head appendages can divert the water carrying the algal cell to the copepod's mouth. Depending on the chemical signals, a freely swimming copepod can orient to capture the cell or turn away if the odor is distasteful.

The feeding current entrains prey but mechanoreceptive predators can not perceive the prey unless the prey move. Since many prey are rheotactic, they will attempt to escape when they detect shear in the fluid velocity gradient (Yen & Fields 1992). Hence, it is advantageous for the predatory copepod to minimize the amount of shear within its feeding current so as not to alert prey to the presence of a predator (Strickler 1982). However, inherent in a feeding current with a steep velocity gradient are areas where shear intensifies and becomes detectable. An interesting interplay results. Prey, entrained within the feeding current, accelerate along the streamlines toward the predator until they try to escape. Weak hops translate the prey but they may become entrained again. Multiple hops of the escaping prey shed multiple jets in the wake. These jets disrupt the structure of the feeding current and intersect mechanoreceptive sensory setae along the antennules, giving information about the size, speed, and position of the prey hopping in the predator's feeding current. With this information, the predator can prepare to lunge suddenly and accurately toward the signal to capture the prey. Hence, the predator's feeding current serves another important function by provoking prey escapes whose jet-like wakes expose their presence. Jet-like fluid mechanical structures are known to elicit responses from mechanosensitive copepods (Yen & Fields 1994). In response to weak jets, the copepod will flick its antennae, a response that can reorient the copepod. When the fluid deformation is of the same velocity and size as a natural wake of a preferred prey, the copepod will strike at the hydrodynamic signal. When the jet speed is further increased, the escape response is elicited. Observations of prey-predator interactions between the copepods *Acartia fossae* and *E. rimana* show that contact does not elicit the capture response; only when *A. fossae* jumps away, shedding a wake against the setae of the predator, does *E. rimana* strike with its maxillipeds (Yen, unpubl. obs).

The feeding current created by a hovering copepod differs in hydrodynamic pattern from the flow field surrounding a free-swimming copepod. When the hovering copepod creates its feeding current, information contained in the cone-shaped volume of water anterior to the copepod is brought past the proximal sensors of the antennules within the central capture region (Fig. 4A). Remaining still in the water and allowing the me-

dium to flow past its sensors, this copepod practices Eulerian averaging of the information input of the medium. For the free-swimming copepod, a column of water anterior to the copepod intersects the array of sensors of the antennules as the copepod moves through the water, now practicing a Lagrangian approach to information gathering (Fig. 4B).

Observations suggest that when signals (such as prey) are abundant, *E. rimana* tends to hover (M. H. Doall and J. Yen, unpubl. obs.). In a food-rich patch, the copepod may hover, scanning the water in close proximity. When the local environment is sparse in food, the copepod swims, seeking food and scanning a volume that projects farther ahead of the copepod than when hovering. Free-swimming may increase encounter rate and serve as the search strategy when food is scarce. These two strategies can adjust the encounter rate of the predator with its prey. Gerritsen & Strickler (1977) proposed an encounter rate model indicating that at different relative swimming speeds, planktonic prey and predators would encounter each other at different rates; fast predators would encounter slow prey while slow predators were more likely to encounter fast moving prey. Their model predicts differences in encounter rate for swimming versus hovering copepods. By adding turbulence (Rothschild & Osborn 1988) and/or random walk (Yamazaki et al. 1991) to this type of encounter model, an increase in encounter probability is predicted. However, little consideration was given to how behavioral responses such as perception are affected by increased fluid motion. Encounter rate in these models is extremely sensitive to slight changes in perceptual abilities. Better estimates are needed of perceptual volume to improve predictions of prey-predator interactions.

Wake structure and intensity

The wakes of a hovering versus swimming versus jumping copepod are different. When a hovering copepod generates its feeding current, the minimum in the velocity gradient occurs near the distal tip of the antennule, demarcating the lateral limit of the feeding current in this region. The hovering copepod pulls in and expels a cloud of fluid. In contrast, in the wake of the freely swimming copepod, the null point occurs more proximal to the tip of the antennule. The swimming copepod leaves barely a trace in the water. As remarked in Yen et al. (1991), a steep velocity gradient minimizes the extent of the hydrodynamic disturbance generated by the copepod, thereby minimizing its conspicuousness. Predators are less likely to encounter the fluctuations caused in the natural flow by the presence of the copepod. For the freely swimming copepod, as the animal generates its flow, it advances into the area from which the water is taken. The flow field is constructed in such a way as to effectively conceal most of the copepod's body: the high velocity zone is directed by the antennal exopods over the body part of most curvature and the inflow of the feeding current matches the forward swimming, movement, resulting in a quiet wake. Only the distal tips of the antennules and caudal setae reveal the path. Such wakes of swimming calanoids dissipate ten times faster than the wakes made by hopping cyclopoids (Strickler 1975a). The flow field is not only shaped so that the sensors are useful, but trimmed to minimize the disturbance.

When an animal moves through water, it creates a disturbance in the fluid. When an animal moves more quickly through water, the energy it leaves in the water is greater, and the fluid pattern persists longer. An escaping copepod moves faster (35–1000 mm s^{-1}) than a swimming copepod (1–10 mm s^{-1}) and hence sheds an intense wake of opposite momentum to the escape. At 1 m s^{-1}, the copepod has a Re of 2000. The copepod thus moves from a laminar regime where viscous forces are dominant into a transition zone where inertial forces become important. We can see in the patterns of the hydrodynamic disturbance that the wake of the quickly moving copepod becomes more turbulent.

In our study, the 30-Hz mushroom-shaped jets shed by the adult copepod looked very different from the trail of smaller circular vortices shed at 100 Hz by the juvenile copepod. The larger wake appears similar to the structure of a toroidal jet. In a study of laminar jet formation as controllable sources of momentum (Voropayev 1983), the vortex dipole is considered the simplest compact vortex structure that has momentum (Voropayev & Afanasyev 1992). Voropayev et al. (1991) further state that "jets and vortex dipoles are united by the same mechanism of generation—the action of a localized source of momentum in a viscous fluid." When the leading edge of the starting jet intrudes into the resting fluid, two vortices of opposite sign—a vortex dipole—forms in the front region. The front region forms the toroidal shape, entraining ambient fluid, while the jet behind flows into the front region. An escaping copepod imparts momentum to the water when it sheds the toroidal jet. By distinguishing differences in the patterns of fluid deformations, other mechanoreceptive animals may recognize the signal source and respond appropriately.

Multiple escapes by the juvenile copepod left a series of vortices. Kinematic analyses show that all 4 vortices were of the same sense (clockwise) as a result of the synchronous movement of the thrusting swimming legs and undulating urosome. This is not a von

Kármán street, which produces vortices of opposing sense (see Vogel 1994, p. 94). According to jet propulsion theory (Weihs 1977), when jets are formed by vortices separated by less than 3 vortex radii as this copepod made, power to the forward movement given by such pulsed jets is greater than that generated by continuous jet propulsion.

Vibrations

Oscillations of reciprocating appendages propel copepods through water. For example, mouthparts oscillate to generate the feeding current and consequent swimming movement. When escape is initiated, the antennules sweep down to the body, then reciprocate and return to their extended positions. During the escape, the urosome rears up, forming a V with the dorsal surface, then pushes posteriorly to resume its initial position. Swimming legs, activated for the escape, are thrust posteriorly. The simultaneous movement of the swimming legs and urosome toward the posterior forces the enclosed volume of water to jet backward, propelling the copepod ahead. The legs relax and feather when they reciprocate back to their original resting position. Repetitive, rapid motion of the swimming legs maintain the high escape velocities of up to 1 m s^{-1} for 3-mm copepods. These oscillations move the fluid as well as the copepod.

Oscillatory fluid movements generated by the reciprocating swimming legs sustain the high flow-speed of water adjacent to the body. At these high Re's, reduction of friction drag may free the copepod from its viscous tether so it can achieve these high speeds (1 m s^{-1} or up to 500 body lengths s^{-1} for adult *E. rimana;* Fields 1996). Multiple thrusts maintain the swimming velocity and allow the copepod to slip speedily along its escape path. At a Re near 2000, the drag coefficient, C_d, can decline abruptly (T. Osborn, pers. comm.). A large reduction in drag may be accomplished with a slight increase in swimming velocity. The copepod's body is streamlined, becoming even more so during the escape, when the antennules lie flat alongside the body and the legs close down onto the narrow urosome. At low Re, streamlining is not needed but at these higher Re's, body form may play an important role in reducing pressure drag.

Hydrodynamic signals have species-specific frequencies. Prey signals include low amplitude, high frequency (1 μm, 40–50 Hz) signals as well as high amplitude, low frequency (3–6 Hz) signals during swimming (Montgomery & Macdonald 1987). The range of frequencies of reciprocating appendages on copepods is 1–150 Hz, even up to 1 kHz for cuticle vibrations (Giguere & Dill 1979). The frequency of vibrations has a size-related component; small copepods have higher frequencies than larger copepods for a variety of movement (Price & Paffenhöfer 1986). Physiological studies show that copepods can detect minute vibrations; the neural response can phase-lock to the frequency of a mechanical stimulus up to 600 Hz (Yen et al. 1992; Lenz & Yen 1993). As mechanoreceptive setae can phase-lock throughout the range of beat frequencies characterizing copepod appendages, detection of the vibratory signal may convey information about the size of the propagator or prey.

Scattered ambient marine noise is within the sensitivity range of a copepod; there is more noise at low frequencies and less noise at frequencies above 500 Hz (Wentz 1962). In the lower frequency range, the threshold displacement of copepods is large, so ambient noise may not be detectable. Above 500 Hz, there is little noise, and the copepod sensory system is more sensitive in this range and can detect smaller-amplitude signals. This similarity in the sensitivity curve of the copepod (Lenz & Yen 1993) and the variations in amplitude of fluid movement of ambient noise suggests that the copepod neural system may act like a matched filter of marine noise, allowing distinct signals to be differentiated above the background noise.

The threshold displacement [M] at each frequency [T^{-1}] in the sensitivity curve can be expressed as the speed [M T^{-1}] at which the displacement occurs. The relationship of threshold speeds versus frequency shows a relatively frequency-independent response; threshold speeds of 20 μm s^{-1} elicit receptor potentials over a range of frequencies. A sharp decrease in sensitivity at 900 Hz implies that time-varying disturbances that occur in less than $1/900^{th}$ s apparently cannot be resolved by the copepod receptor system. Still, the copepod receptor system is remarkably acute: copepods can sense less than 10 nm of displacement of their setae at 20 μm s^{-1} velocities. These thresholds are similar to those determined for other aquatic crustaceans. A 10-nm displacement of caudal fan setae elicits responses in crayfish (Moss & Wiesenfeld 1995) and the mean threshold pulse speed for a cladoceran is 0.36 μm s^{-1} (Zaret 1980).

Giguere & Dill (1979) claimed that copepods produce acoustic stimuli from 500 to 1200 Hz, recorded from copepods glued to radio earphones. Kirk (1985) discounted these as cuticle vibrations. As acoustic tuning is determined by the mechanical properties of the sensor (Freeman & Weiss 1988), perhaps the cuticle of the setal sensor or a seta of a given size have mechanical resonances around 900 Hz. Since different species of copepods can have chitinous setal sensors of similar size, this common physical trait of the sen-

sory system may account for the similar sensitivity of the receptors of the copepod antennule to unnaturally high frequencies. Further analyses (Yen, unpubl.) of the behavioral responses elicited by the vibrations may show that *E. rimana* exhibits mixed responses, not a consistent one, suggesting that this high frequency signal conveys no information and simply startles the animal.

Many other aquatic animals can sense similar vibrations. Quantitative studies by Bleckmann et al. (1991) show that hydrodynamic receptor systems in a variety of animals are well adapted to the frequency content of naturally occurring hydrodynamic stimuli. The hair fan organs on the chelae and carapace of the lobster *Homarus gammarus* L. are extremely sensitive to oscillatory patterns of water flow, at frequencies up to 100 Hz (Laverack 1962). Water-movement sensitive setae on the chelae of the crayfish *Cherax destructor* are most sensitive to oscillations of 150–300 Hz with a water particle displacement threshold of about 0.2 μm (Tautz & Sandeman 1980). Sensory setae on the telson of the crayfish *Procambarus clarkii* has a threshold of 0.1 μm at 100 Hz (Wiese 1976). Weatherby et al. (1994) remarked that the setae of copepods are morphologically similar to sensors known from these descriptive studies of larger crustaceans. Backswimmers, *Notonecta*, discriminate prey from nonprey on the basis of the frequency content of the water vibrations produced by members of these two groups (Wilcox 1988). Tuning curves of spiders indicated that the vibration-sensitive neurons behave like bandpass filters in which the best frequencies are in the frequency range of courtship and prey signals encountered by the spider in its natural habitat (Speck-Hergenröder & Barth 1987). The attack response by a chaetognath was triggered at frequencies between 9 and 20 Hz at source amplitudes of 100–500 μm (Horridge & Boulton 1967), which Newbury (1972) found to correspond to the beat frequencies of the feeding appendages of certain copepods in their diet. More studies of how organisms acquire and respond to information are needed to improve our understanding of their sensory ecology (Dusenbery 1992).

Information comes to these animals in different ways. For the lobster and crayfish, their chemical cues often are carried in turbulent plumes, resulting in a chaotic and patchy distribution of signals. It is difficult to follow an odor path to the source; sensors detect signals and monitor flow direction. In contrast, information content and signal transmission to the copepod, spider, and backswimmer have been simplified. In the low-Re regime of the copepod flow field, viscosity reduces turbulent motion into laminar shear. Signals, caught in the laminar feeding current, are perceived as a disruption of a defined pattern. Hence, the complexity of information flow to the copepod from the ambient fluid motion is simplified within the dynamic yet laminar feeding current. The spider does not monitor all signals in its surroundings, only those that vibrate the web, thus confining the information flow from the 3-dimensional environment to a 2-dimensional web. Similarly, by living at the air-water interface, the backswimmer detects signals only on a 2-dimensional plane. In these different ways for these different animals, the complexity of information content found in their natural surroundings has been reduced.

Conclusions

The velocity gradient defining the distinct hydrodynamic patterns found in the copepod feeding current, wake, and pulsed flow can change quickly over time and space. The copepod sensory system provides the tools needed to sense such small-scale flow containing both positional and temporal information. Separation between individual sensory setae and the tufts of setae at the distal tips of the antennules provide the copepod with the ability to measure shear at length scales as fine as tens of micrometers and up to 10 millimeters, respectively. Only 10 nm of displacement at 20 μm s^{-1} are needed to elicit a physiological response from the linear array of multidirected setae. Latencies of less than 10 ms in the reaction times of the neurophysiological response and phase locking to oscillations over 200 Hz indicate that copepods can respond to rapid changes in water motion. Copepods capture prey at reaction distances of 1–2 body lengths. Hence, the sensitivity of the sensors and the spacing, orientation, and morphology of the receptors permit sensing of water motion on the microscale. Copepod behavior can be used quantitatively as the criterion for detection of the hydrodynamic signal. Thus, copepods are useful not only as fish food but also as indicators of the structure of small-scale fluid motion.

The Re of the feeding current of copepods is less than 1. The Re of swimming by copepods is around 2–20. The Re of escaping is around 2000. The Re of these activities of copepods span an interesting transition zone, from a low Re, viscosity-limited realm to an intermediate-to-high Re, inertia-sensitive realm. Copepods have evolved to be just the right size (0.3–10 mm long) and speed to utilize the physical structure of water at this interface for their advantage. With the feeding current, copepods modify water flow around themselves, enhancing their perception of important cues. As a low-Re structure, the feeding current organizes flow into a neat laminar pattern to facilitate signal detection above the background noise. When

copepods use the muscles in their antennules, legs, and urosome to initiate the rapid escape, they assume a streamlined form and are able to achieve speeds of 1 m s^{-1}, shedding wakes in the form of jets and vortices. By studying copepods, perhaps we can learn more about the flow patterns of water at this poorly-understood transition zone between laminar and turbulent regimes.

Acknowledgments. We would like to thank Drs. Rick Tankersley and Evan Ward for inviting us to participate in their exciting symposium. We also wish to thank the following people for their contributions: Dr. David Fields for providing the detailed analysis of the flow field of *Euchaeta rimana*. Michael Doall for his help in the laboratory, Dr. Marc Weissburg for his help with the color photo-layouts. We appreciate the help from the people in our laboratories at that time: John Reimer, Ladina Lutz, Beth Williams, and Dr. Grazia Mazzochi. We also appreciate the critical comments of Drs. Alexander, LaBarbera, Shimeta, and Weissburg in their reviews of the manuscript. JY would like to thank the Office of Naval Research (contracts N00014-92-J1690, N00014-94-10696), and JY and JRS would like to thank the National Science Foundation (OCE 9314934) for funding this research. This is contribution #1029 from the Marine Sciences Research Center. This article is dedicated to the memory of our colleague and dear friend, Dr. Akira Okubo. His ability to define the complexities of fluid dynamics came from a depth of knowledge and understanding that we strive to gain.

References

Alcaraz M & Strickler JR 1988. Locomotion in copepods: pattern of movements and energetics of *Cyclops*. Hydrobiologia 167/168: 404–414.

Andrews JC 1983. Deformation of the active space in the low Reynolds number feeding current of calanoid copepods. Can. J. Fish. Aquat. Sci. 40: 1293–1302.

Batchelor GK 1967. An Introduction to Fluid Dynamics. Cambridge Univ. Press, Cambridge, UK. 615 pp.

Bleckmann H, Breithaupt T, Blickhan R, & Tautz J 1991. The time course and frequency content of hydrodynamic events caused by moving fish, frogs, and crustaceans. J. Comp. Physiol. A. 168: 749–757.

Boxshall GA, Yen J & Strickler JR, in press. Functional significance of the sexual dimorphism in the cephalic appendages of *Euchaeta rimana* Bradford. Bull. Mar. Sci.

Buskey EJ 1984. Swimming pattern as an indicator of the roles of copepod sensory systems in the recognition of food. Mar. Biol. 78: 53–57.

Chacon-Barrientos Y 1980. Ultrastructure of sensory units on the first antennae of calanoid copepods. M.S. thesis, Univ. Ottawa, Canada. 81 pp.

Costello JH, Strickler JR, Marrase C, Trager G, Zeller R, & Freise AJ 1990. Grazing in a turbulent environment: behavioral response of a calanoid copepod, *Centropages hamatus*. Proc. Natl. Acad. Sci. USA 87: 1648–1652.

Doall MH 1995. The components of predation between *Euchaeta rimana*, a predatory calanoid copepod, and smaller copepod species. M.S. thesis, State Univ. of New York at Stony Brook. 78 pp.

Dourdeville TA 1981. A physical and physiological analysis of near-field displacement reception by a calanoid copepod. *Centropages typicus* Kroyer. M.A. thesis. Boston Univ. 186 pp.

Dusenbery DB 1992. Sensory Ecology. How Organisms Acquire and Respond to Information. W. H. Freeman and Co., New York. 558 pp.

Fields DM 1996. Interactions of marine copepods with a moving fluid environment. Ph.D. thesis, State Univ. of New York at Stony Brook. 403 pp.

Fields DM & Yen J 1993. Outer limits and inner structure: the 3-dimensional flow fields of *Pleuromamma xiphias*. Bull. Mar. Res. 53: 84–95.

Folt C & Goldman CR 1981. Allelopathy between zooplankton: a mechanism for interference competition. Science 213: 1133–1135.

Freeman DM & Weiss TF 1988. The role of fluid inertia in mechanical stimulation of hair cells. Hearing Res. 35: 201–208.

French AS 1988. Mechanotransduction. Ann. Rev. Physiol. 54: 135–152.

Friedman MM 1980. Comparative morphology and functional significance of copepod receptors and oral structures. In: Evolution and Ecology of Zooplankton Communities. Kerfoot WM, ed., pp. 185–197. University Press of New England, Hanover, New Hampshire.

Gerritsen J & Strickler JR 1977. Encounter probablities and community structure in zooplankton: a mathematical model. J. Fish. Res. Bd. Canada 34: 73–82.

Giguere LA & Dill LM 1979. The predatory response of *Chaoborus* larvae to acoustic stimuli, and the acoustic characteristics of their prey. Z. Tierpsychol. 50: 113–125.

Gill CW & Poulet SA 1986. Utilization of a computerized micro-impedence system for studying the activity of copepod appendages. J. Exp. Mar. Biol. Ecol. 101: 193–198.

Haury LR, Kenyon DE, & Brooks JR 1980. Experimental evaluation of the avoidance reaction of *Calanus finmarchicus*. J. Plankt. Res. 2: 187–202.

Horridge GA & Boulton PS 1967. Prey detection by Chaetognatha via a vibration sense. Proc. Roy. Soc. B. 168: 413–419.

Huys R & Boxshall GA 1991. Copepod Evolution. Ray Society, Unwin Brothers, London, England. 468 pp.

Hwang J-S, Costello JH, & Strickler JR 1994. Copepod grazing in turbulent flow: elevated foraging behavior and habituation of escape responses. J. Plankt. Res. 16: 421–431.

Jansson J, Coombs S, & Pride S 1990. Feeding and orientation of mottled sculpin, *Cottus bairdi*, to water jets. Env. Biol. Fishes 29: 43–50.

Jonsson PR & Tiselius P 1990. Feeding behavior, prey detection and capture efficiency of the copepod *Acartia tonsa* feeding on planktonic ciliates. Mar. Ecol. Progr. Ser. 60: 35–44.

Kerfoot WC, Kellogg DC, Jr., & Strickler JR 1980. Visual observations of live zooplankters: evasion, escape and

chemical defenses. In: Evolution and Ecology of Zooplankton Communities. Kerfoot WM, ed., pp. 10–27. University Press of New England, Hanover, New Hampshire.

Kiørboe T & Saiz E 1995. Planktivorous feeding in calm and turbulent environments, with emphasis on copepods. Mar. Ecol. Prog. Ser. 122: 135–145.

Kirk KL 1985. Water flows produced by *Daphnia* and *Diaptomus*: implications for prey selection by mechanosensory predators. Limnol. Oceanogr. 30: 679–686.

Koehl MAR & Strickler JR 1981. Copepod feeding currents: food capture at low Reynolds number. Limnol. Oceanogr. 26: 1062–1073.

Laverack MS 1962. Responses of cuticular sense organs of the lobster *Homarus vulgaris* (Crustacea). I. Hair-pegs organs as water current receptors. Comp. Biochem. Physiol. 5: 319–325.

Lazier JRN & Mann KH 1989. Turbulence and diffusive layers around small organisms. Deep-Sea Res. 36: 1721–1733.

Lenz PH & Yen J 1993. Distal setal mechanoreceptors of the first antennae of marine copepods. Bull. Mar. Res. 53: 170–179.

Mann KH & Lazier JRN 1991. Dynamics of Marine Ecosystems. Biological-Physical Interactions in the Oceans. Blackwell Scientific Publ., Cambridge, MA. 466 pp.

Markl H 1978. Adaptive radiation of mechanoreception. In: Sensory Ecology Reviews and Perspectives. Ali MA, ed., pp. 319–344. Plenum Press, New York.

Marrasé C, Costello JH, Granata T, & Strickler JR 1990. Grazing in a turbulent environment: II. Energy dissipation, encounter rates and efficacy of feeding currents in *Centropages hamatus*. Proc. Natl. Acad. Sci. USA 87: 1653–1657.

Montgomery JC & Macdonald JA 1987. Sensory tuning of lateral line receptors in antarctic fish to the movements of planktonic prey. Science 235: 195–196.

Moore PA, Fields DM, & Yen J 1994. The fine scale structure of chemical signals within the feeding current of calanoid copepods. (Abstr.) EOS, Trans. Am. Geophys. Union 75: 163.

Moss F & Wiesenfeld K 1995. The benefits of background noise. Sci. Am. (August 1995): 66–69.

Newbury TK 1972. Vibration perception by chaetognaths. Nature 236: 459–460.

Osborn TR 1996. The role of turbulent diffusion for copepods with feeding currents. J. Plankt. Res. 18: 185–195.

Price HJ & Paffenhöfer G-A 1986. Effects of concentration on the feeding of a marine copepod in algal monocultures and mixtures. J. Plank. Res. 8: 119–128.

Rothschild BJ & Osborn TR 1988. Small-scale turbulence and plankton contact rates. J. Plankton Res. 10: 465–474.

Speck-Hergenröder J & Barth FG 1987. Tuning of vibration sensitive neurons in the central nervous system of a wandering spider, *Cupiennius salei* Keys. J. Comp. Physiol. A160: 467–475.

Squires KD & Yamazaki H 1993. Towards direct numerical simulation of zooplankton interaction with homogenous turbulence. Spec. Rept. No. 45, Center for Great Lakes Research, Univ. Wisconsin-Milwaukee. 48 pp.

Stein MA, Okubo A, & Yen J 1994. A mathematical model of the copepod feeding current: a fluid dynamical approach. (Abstr.) EOS, Trans. Am. Geophys. Union 75: 163.

Strickler JR 1975a. Swimming of planktonic *Cyclops* (Copepoda, Crustacea): pattern, movements and their control. In: Swimming and Flying in Nature, Vol. 2. Wu TY, Brokaw CJ, & Brennan C, eds., pp. 599–616. Plenum Press, New York.

——— 1975b. Intra- and interspecific information flow among planktonic copepods: receptors. Verh. Int. Ver. Limnol. 19: 2951–2958.

——— 1977. Observation of swimming performances of planktonic copepods. Limnol. Oceanogr. 22: 165–169.

——— 1982. Calanoid copepods, feeding currents, and the role of gravity. Science 218: 158–160.

——— 1984. Sticky water: a selective force in copepod evolution. In: Trophic Interactions within Aquatic Ecosystems. AAAS Symp. 85. Meyers DG & Strickler JR, eds., pp. 187–239. Westview Press, Inc, Boulder, Co.

——— 1985. Feeding currents in calanoid copepods: two new hypotheses. Soc. Exp. Biol. 1985: 459–485.

Strickler JR & Bal AK 1973. Setae of the first antennae of the copepod *Cyclops scutifer* (Sars): their structure and importance. Proc. Nat. Acad. Sci. USA 70: 2656–2659.

Strickler JR & Hwang J-S 1996. Matched spatial filters in long working distance microscopy of phase objects. In: Focus on Modern Microscopy. Cheng PC, Hwang PP, Wu JL, Wang G, & Kim H, eds. World Scientific Publ., River Edge, NJ (in press).

Strickler JR & Twombly S 1975. Reynolds number, diapause, and predatory copepods. Verh. Int. Ver. Limnol. 19: 2948–2950.

Strickler JR, Ono D, & Reimer J 1995. Spatial filtering in microscopy: the use of matched filters to see further in time and space. Zool. Studies 34 (suppl. 1): 227–228.

Tautz J 1979. Reception of particle oscillation in a medium—an unorthodox sensory capacity. Naturwiss. 66: 452–461.

Tautz J & Sandeman DC 1980. The detection of waterborne vibration by sensory hairs on the chelae of the crayfish. J. Exp. Biol. 88: 351–356.

Teyke T 1988. Flow field, swimming velocity and boundary layer: parameters which affect the stimulus for the lateral line organ in blind fish. J. Comp. Physiol. A163: 53–61.

Van Dyke M 1981. An Album of Fluid Motion. The Parabolic Press, Stanford, CA. 176 pp.

Vogel S 1994. Life in Moving Fluids. 2nd edition. Princeton University Press, Princeton, NJ. 467 pp.

Voropayev SI 1983. Free jet and frontogenesis experiments in shear flow. Tech. Rep. Woods Hole Oceanogr. Inst. WHOI-83-41: 147–159.

Voropayev SI & Afanasyev YD 1992. Two-dimensional vortex-dipole interactions in a stratified fluid. J. Fluid Mech. 236: 665–689.

Voropayev SI, Afanasyev YD, & Filippov IA 1991. Hori-

zontal jets and vortex dipoles in a stratified fluid. J. Fluid Mech. 227: 543–566.

Weatherby TM, Wong KK, & Lenz PH 1994. Fine structure of the distal sensory setae on the first antennae of *Pleuromamma xiphias* Giesbrecht (Copepoda). J. Crust. Biol. 14: 670–685.

Weihs D 1977. Periodic jet propulsion of aquatic creatures. Fortschr. Zool. 24: 171–175.

Wentz GM 1962. Acoustic ambient noise in the ocean: spectra and sources. J. Acoust. Soc. America 34: 1936–1956.

Wiese K 1976. Mechanoreceptors for near-field water displacements in crayfish. J. Neurophysiol. 39: 816–833.

Wilcox S 1988. Surface wave reception in invertebrates and vertebrates. In: Sensory Biology of Aquatic Animals. Atema J, Fay RR, Popper AN, and Tavolga WN, eds., pp. 644–663. Springer-Verlag, New York.

Wong CK 1996. Responses of copepods to hydromechanical stimuli. Crustaceana, in press.

Yamazaki H, Osborn TR, and Squires KD 1991. Direct numerical simulation of planktonic contact in turbulent flow. J. Plankt. Res. 13: 629–643.

Yen J 1982. Sources of variability in attack rates of *Euchaeta elongata* Esterly, a carnivorous marine copepod. J. Exp. Mar. Biol. Ecol. 63: 105–117.

——— 1983. Effects of prey concentration, prey size, predator life stage, predator starvation and season on predation rates of the carnivorous marine copepod *Euchaeta elongata*. Mar. Biol. 75: 69–77.

——— 1985. Selective predation by the carnivorous marine copepod *Euchaeta elongata:* laboratory measurements of predation rates verified by field observations of temporal/spatial feeding patterns. Limnol. Oceanogr. 30: 577–595.

——— 1988. Directionality and swimming speeds in predator-prey and male-female interactions of *Euchaeta rimana*, a subtropical marine copepod. Bull. Mar. Sci. 43: 175–193.

——— 1991. Predatory feeding behavior of an antarctic marine copepod, *Euchaeta antarctica*. In: Proceedings of the Pro Mare Symposium on Polar Marine Ecology. Sakshaug E, Hopkins CCE, & øritsland NA, eds. Polar Res. 10: 433–442.

Yen J & Fields DM 1992. Escape responses of *Acartia hudsonica* nauplii from the flow field of *Temora longicornis*. Arch. Hydro. Beih. 36: 123–134.

——— 1994. Behavioral responses of *Euchaeta rimana* to controlled fluid mechanical stimuli. (Abstr.) EOS, Trans. Am. Geophys. Union 75: 184.

Yen J & Nicoll NT 1990. Setal array on the first antennae of a carnivorous marine copepod *Euchaeta norvegica*. J. Crust. Biol. 10: 327–340.

Yen J, Sanderson BG, Strickler JR, & Okubo A 1991. Feeding currents and energy dissipation by *Euchaeta rimana*, a subtropical pelagic copepod. Limnol. Oceanogr. 36: 362–369.

Yen J, Lenz PH, Gassie DV, & Hartline DK 1992. Mechanoreception in marine copepods: electrophysiological studies on the first antennae. J. Plankt. Res. 14: 495–512.

Zaret RE 1980. Zooplankters and their interactions with water, with each other, and with their predators. Ph.D. thesis, Johns Hopkins Univ., Baltimore. 166 pp.

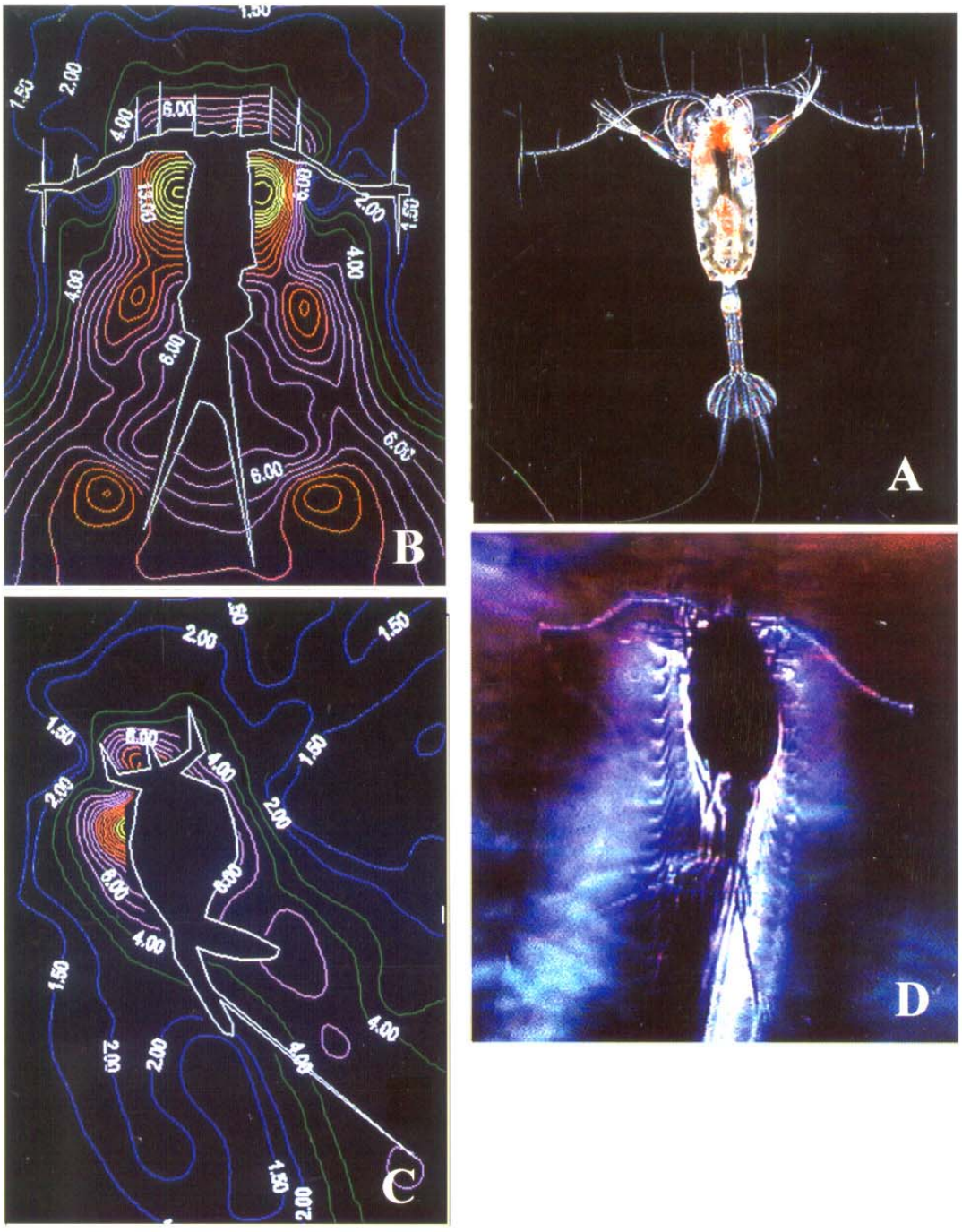

Fig. 2. A. Photomicrograph of a live copepod, *Euchaeta norvegica*, showing the breadth of the extended maxillipeds, capture appendages of this pelagic marine carnivore (cephalothorax ~4 mm long). Note the long setae lining the antennules, the pair of very long caudal setae, and the setae imparting iridescence to the caudal fan. Maturing oocytes within the paired

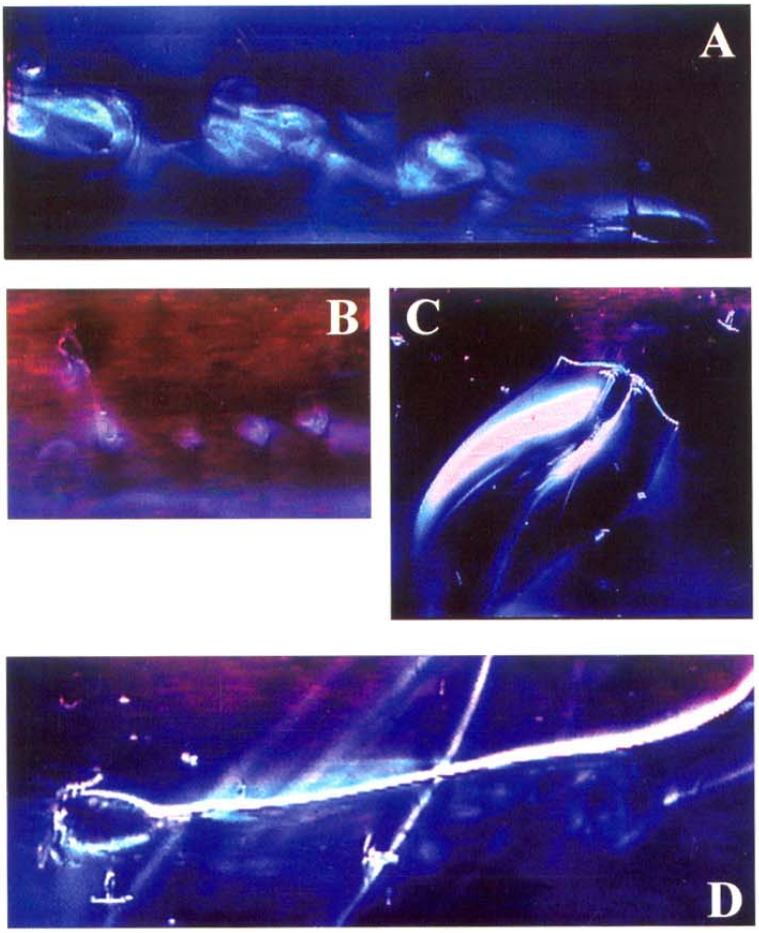

Fig. 3. A. Three toroidal vortices (30 Hz) shed by the escape movements of an adult copepod, *Euchaeta rimana* (cephalothorax 2.4 mm long; copepod is the dark silhouette in the lower right corner). **B.** Four vortices (100 Hz) of clock-wise sense shed by the escape movements of a juvenile copepod, *E. rimana* (cephalothorax 1.5 mm long; copepod is seen in profile in the upper left area of the videoimage). **C** and **D.** Wakes of free-swimming copepods, *E. rimana* (cephalothorax 2.4 mm long), swimming through seawater. **C.** Plan view of copepod swimming upward. **D.** Profile view of copepod swimming to the left. Note how smooth and thin the hydrodynamic trail is. The density gradient in the seawater, necessary for Schlieren photography, is enhanced visually with the color gradient. The white image shows the water moved by the copepod into an adjacent layer of water of differing density.

signal is that of a predator. Like a spider and its web, the copepod and its feeding current can be examined as a unit, as recommended by Strickler (1985). Vibrations transmitted along the web inform the spider of the position of the signal source within its web. Signals entrained along the streamlines and intersecting certain receptors inform the copepod of the position of the source within the volume of its feeding current.

Within the copepod feeding current, flow velocities remain relatively stable. Using metabolic energy to

---

←

oviducts in the translucent body of the copepod are deep blue. **B** and **C.** Isotachs (lines of equal speed) of fluid flow surrounding a tethered copepod, *Euchaeta rimana* (cephalothorax 2.4 mm long). Each isoline represents increments of 1 mm s^{-1} of flow speed (except for the 1.5 to 2.0 mm s^{-1} isolines). **B.** Dorsal view of flow: The innermost yellow isoline of the plan view represents a maximum velocity of 20 mm s^{-1}. The blue isoline crossing the distal tip of each antennule represents 1.5 mm s^{-1} flow. These are separated by only 2 mm. **C.** Lateral view of the flow: The innermost yellow isoline on the dorsal side of the copepod body (at left) represents 17 mm s^{-1} flow. **D.** Schlieren videoimage of *Pareuchaeta* sp. showing the hydrodynamic imprint left by oscillatory movements of the locomotory appendages, the second antennae. The frequency of the movement is 30 Hz. The distance between ripples (9 ripples per cephalothorax length) is approximately 500 μm. The density gradient in the seawater, necessary for Schlieren photography, is enhanced visually with the color gradient. The white image shows the water moved by the copepod into an adjacent layer of water of differing density.